Substrate-Integrated-Waveguide Power Dividers

An overview of the current technology.

Shahriar Hasan Shehab, Nemai Chandra Karmakar, and Jeffrey Walker

Power dividers are important components of microwave/millimeter wave (mm-wave) circuit design. This article provides a comprehensive review of the state-of-the-art substrate-integrated-waveguide (SIW) power dividers/combiners. SIW technology converts waveguide-like structures into planar form, compensates for the drawbacks of microstrip structures at higher-frequency circuit designs, and minimizes production complexity and costs compared to conventional waveguide structures. An overview of how traditional dividers have progressive adopted the SIW technique is presented and a comparative performance analysis of the divider types and practical paradigm show the future potential of SIW technology.

SIW TECHNOLOGY

Power dividers are the fundamental building blocks for microwave and mm-wave integrated circuits, such as multiplexers, power combiners, mixers, and antenna feed networks. Power dividers are usually reciprocal devices; they operate by both dividing and combining power in a specific manner based on the requirements. Power-divider design comprises lower attenuation and phase balancing, which have been core requirements as well as challanges for designers. Essential performance parameters for power-divider design are listed in Figure 1. This article presents a comprehensive review of the different SIW power dividers and their progressive development.

Digital Object Identifier 10.1109/MAP.2019.2943308
Date of current version: 15 October 2019

Conventional rectangular waveguides are a widely accepted technology due to their higher quality (Q) factor (5,000–10,000), low loss at microwave range, and high power-handling capability. However, their cumbersome structure requires mechanical assembling, which makes it difficult and expensive to integrate them with microwave and mm-wave monolithic integrated circuits. Conversely, planar microstrip configuration provides tremendous structural compactness, high Q factor (50–100) [1], and transition networks, which have more design flexibility and cost effectiveness. Nevertheless, at higher frequencies, microstrip lines have significant radiation leakage, which increases the insertion loss and, eventually, reduces the divider efficiency. Additionally, a scientific drawback of mictrostrip technology is that the linewidth becomes unrealizably thin for large power-division ratios, as are required in large antenna array beam tapering. Due to the growing interest in developing mm-wave circuit components, there is a significant technological gap that has the advantages of low loss and planar configuration. The SIW technology was first proposed through a patent [2] in 1994, which synthesized the metallic waveguides into a planar form by inserting metallic rows of vias/conducting cylinders as an electric sheild to replace metal plates. The traditional low-cost printed circuit board (PCB) process is applicable for fabrication and demonstrates the potential of designing high-Q (500–1,000) multiport components. This technology has established a dynamic bridge between conventional waveguides and microstrips, eliminating both of their drawbacks. A complete antenna array system incorporated with the SIW feeding technique first came onboard in 1998 [3]. Since then, research interest has grown signifcantly for the use of SIW technology in mm-wave circuit component developments.

The aim of this article is to review various SIW power-divider topologies, including corporate, series, multimode interference (MMI), half-mode (HM) SIW (HMSIW), magic-T, radial cavity, Wilkinson, and Gysel, and their developments over the past years. Multistage reflection reduction, bandwidth enhancement, and structural compactness were the main focuses of this investigation.

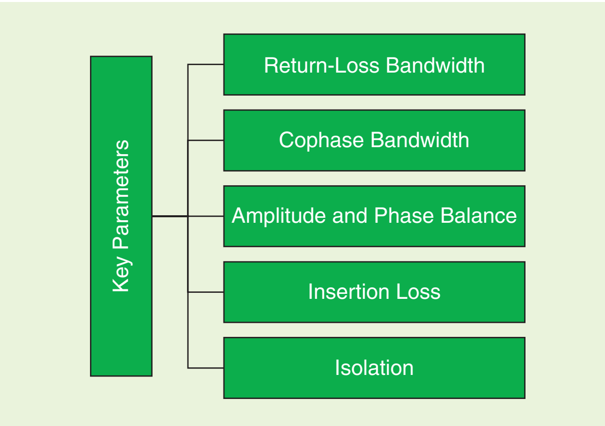

FIGURE 1. The performance indicators for power-divider design.

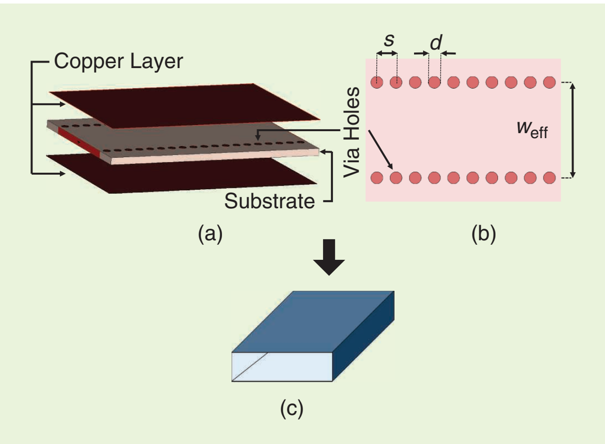

FIGURE 2. The SIW configuration: (a) side view, (b) top view, and (c) equivalent rectangular waveguide.

SIW DESIGN PRINCIPLE

A regular SIW structure incorporated with conducting cylinders as vias connecting the top and bottom copper layers of a substrate material is shown in Figure 2. Here, d is the via diameter, s is the spacing between adjacent vias, and w is the equivalent rectangular waveguide width. First, the SIW structure needs to be converted into an equivalent rectangular waveguide; then, the fundamental theory of conventional rectangular waveguides can be applied in the SIW structure. Such an SIW structure functions like an equivalent rectangular waveguide and delimits the transverse-electric (TE) wave propagation mode, which is in a planar form. Therefore, the formula for the cutoff frequency can be written as [4]

$$f_{c_{mn}} = \frac{1}{2\pi\sqrt{\varepsilon\mu}}\sqrt{\left(\frac{m\pi}{a}\right)^2+\left(\frac{n\pi}{b}\right)^2}, \tag{1}$$

where m and n refer to the half-wave variations in the x and y directions, respectively; ε and μ are the substrate material permittivity and permeability, respectively; a is the width, which is w_{eff}; and b is the substrate thichness in this case. For TE_{10} as the dominant mode,

$$f_{c10} = \frac{c}{2w_{\text{eff}}\sqrt{\varepsilon_r}}. \tag{2}$$

Equation (2) can be solved for the effective SIW width (w_{eff}) for a particular frequency, which leads to the width of the equivalent rectangular waveguide (w). One of the widely accepted equations for calculating w_{eff} derived using the full-wave finite element method (FEM) can be written as [5]

$$w_{\text{eff}} = w - 1.08\left(\frac{d^2}{s}\right)+0.1\left(\frac{d^2}{w}\right). \tag{3}$$

Therefore, the guided wavelength can be determined by

$$\lambda_g = \frac{\lambda_o}{\sqrt{\varepsilon_r(1-(f_c/f_o)^2)}}, \tag{4}$$

where f_o is the antenna operating frequency. The SIW cutoff frequency needs to be chosen by considering the single mode of operation. The dispersion characteristics of the SIW are similar to rectangular waveguide at the dominant mode (TE_{10}) [6]. An example using Taconic TLX-8 as the substrate material ($\varepsilon_r = 2.55$ and $\tan\,\delta = 0.0019$) with a cutoff frequency of 12.5 GHz is designed. The s/d ratio is chosen to be below 2 ($s = 0.8$ and $d = 0.5$) to minimize the radiation leakage, as suggested in [5]. The S-parameter responses are shown in Figure 3, where the return loss (S_{11}) goes below –10 dB at 12.5 GHz onward. According to the classical waveguide theory, such a structure should remain in the dominant mode until 25 GHz, at which point the second, higher mode (i.e., TE_{20}) starts.

SIW POWER DIVIDERS

Since the first work on SIW (called *laminated waveguide* and presented in [3] and [7]), the SIW H-plane T- and Y-junctions were reported in [8] for K_a-band applications. Both junctions have included inductive posts to improve reflections from the port. In the Y-junction, the feeding waveguide width was optimized to obtain the TE_{10} mode excitation only within the desired frequency band. Additionally, simulation and measured results showed that the Y-junction provides a wider bandwidth of 25.2% compared to the T-junction, which was at 10.2%. This section will describe the different SIW power dividers shown in Figure 4 and their individual progressive developments.

CORPORATE (TREE) DIVIDERS

Corporate feed structures have the merit of delivering both equal and unequal splits with higher cophase bandwidth. Although insertion loss is expected to be higher because the signal needs to travel a longer distance, higher bandwidth can be achieved. SIW corporate dividers are capable of delivering lower loss designs at higher frequency with the planar configuration. The following section discusses the development of single- and multilayer configurations.

SINGLE-LAYER CONFIGURATIONS

A 16-way equal-split SIW corporate feed network was proposed in [9] for X-band applications. The proposed structure was formed by several SIW bends and the T- and Y-junctions, as shown in Figure 5. The optimization process followed the guidelines from [8]. The designed feed network was utilized in an antipodal linearly tapered slot antenna array design [10].

An eight-way SIW corporate power divider consisting of only Y-junctions was reported in [11] for K_u-band applications. An inductive post was replaced at the SIW bends with a right-angle bend, as shown in Figure 6(b). The tilt angle and length were optimized to obtain lower reflection for better impedance matching. The return loss was found to be less than –20 dB throughout the operational bandwidth, but the size seemed to be at least twice that of the regular size. A similar method was applied in the

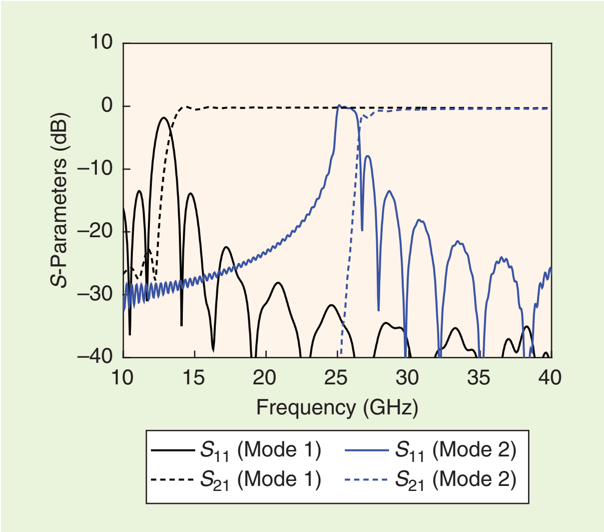

FIGURE 3. The S-parameter response of the SIW transmission line.

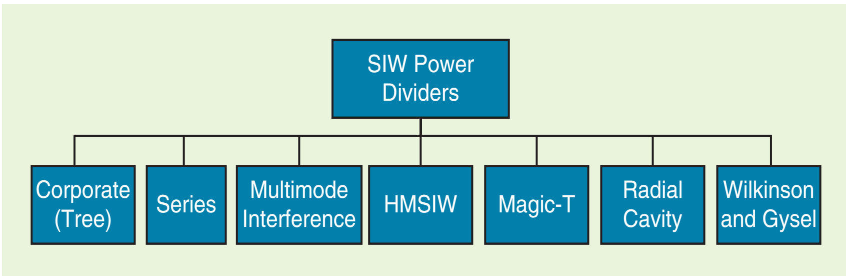

FIGURE 4. The classifications of SIW power dividers.

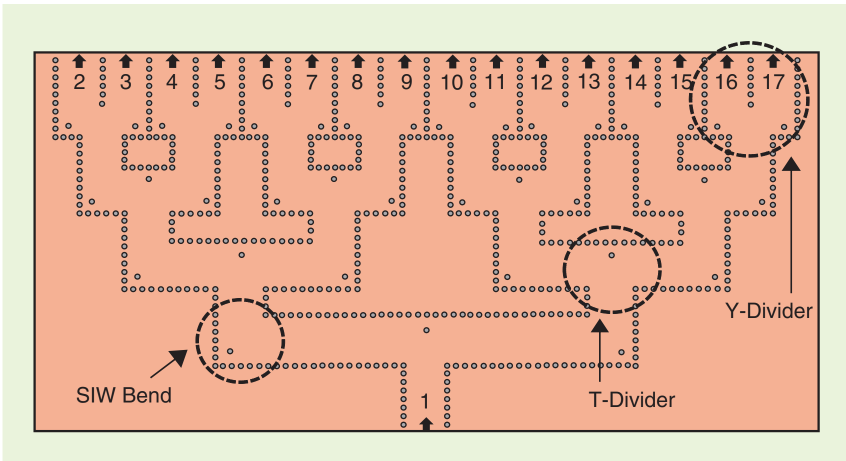

FIGURE 5. A 16-way single-layer SIW corporate divider configuration.

design of a four-way power splitter at the C-band [12]. The proposed power splitter rendered a wide bandwidth of approximately 40% from 4.5 to 6.8 GHz. However, amplitude and phase mismatches were observed at different ports over the operating bandwidth. A four-way power divider for a 1 × 4 dual-dipole array antenna was reported in [13]. The design configuration adapted conventional design techniques, but it implemented a swept-arc bend instead of the commonly used right-angle bend for lowering reflection from the waveguide discontinuities, as shown in Figure 6(c). Although the design and optimization of such a swept bend were complex compared to the previously reported works, the proposed power divider improved the bandwidth to approximately 53%. The SIW corporate power-divider structure has also been implemented in a monopulse array antenna design at the K_a-band [14]. In [14], a four-way power divider was designed with a right-angle bend topology. Furthermore, another monopulse antenna array was proposed in [15] at the W-band. At such a high frequency, the SIW width became so narrow (1.76 mm) that the accomodation of another reflection-cancelling post within the T-junction was impossible with the conventional PCB process. To address that design problem, the T-divider was modified as shown in Figure 7. At the first modification, the junction behaved as a resonator and degraded the overall bandwidth. Nevertheless, the second modification improved the return loss and produced a wider bandwidth of approximately 5.8% without any additional post.

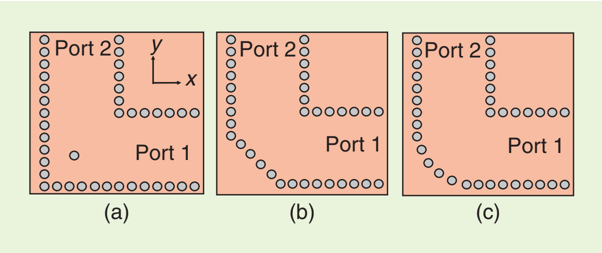

FIGURE 6. The types of SIW bends: (a) inductive posts, (b) right angle, and (c) swept arc.

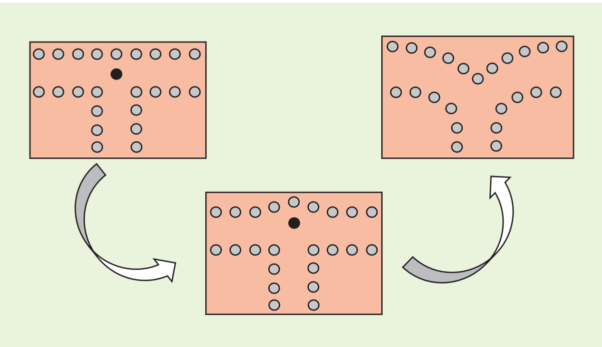

FIGURE 7. A T-junction improvisation.

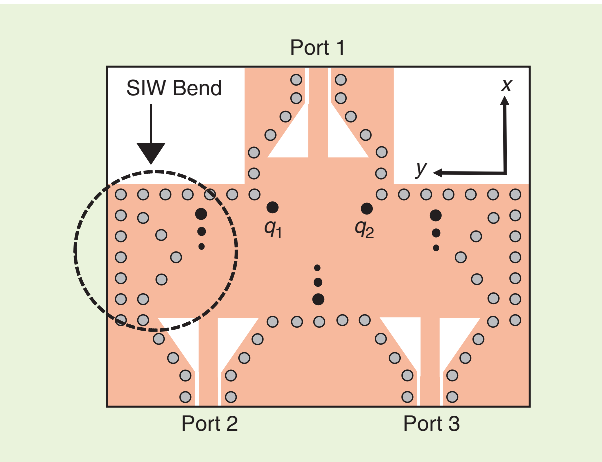

FIGURE 8. The modified T-junctions.

A novel concept for a wideband power-divider design was presented in [16] and introduced improvements on the T- and Y-junction designs. The T- and Y-junctions achieved 63% and 40% bandwidth, respectively, with lower insertion loss. Impressive cophase bandwidth was obtained with fewer than ±4° and ±0.9-dB phase and amplitude imbalances over the operating bandwidth. The proposed T-divider shown in Figure 8 consists of multiple inductive posts with a gradual increase in diameter to obtain better input impedance matching. Additionally, two more posts, q_1 and q_2, were added to minimize the capacitive effect due to the discontinuity at the bends, with their positions and diameters optimized for better matching. Similarly, three posts were added in the SIW bend, and a triangular extension of the short via wall was introduced at the corner to lower reflection. The Y-junction followed a simiar topology. Utlizing this design, an ultrawideband Vivaldi antenna array, which showed a very satisfactory patterned bandwidth in both E- and H-planes, was reported in [17]. The proposed modified power-divider design is a facinating option except for the design complexity, which might be an issue for large-scale power-splitter designs.

Another two-way Y-splitter was presented in [18] for S-band applications. The proposed divider provided 57% bandwidth from 2 to 3.6 GHz with an insertion loss of approximately 0.4 ± 0.2 dB. The two-way Y-divider proposed in [19] showed a similar structure but applied a step transition network instead. The proposed design depicted a comparatively lower bandwidth of 5.7% with an insertion loss of 0.5 ± 0.5 dB. Moreover, the conventional T-junction design was improved by introducing a single-ridge structure in [20]. The ridge waveguide structure has a wider separation between the two adjacent mode cutoff frequencies, which helped with the bandwidth enhancement. The overall bandwidth of the proposed design was improved by 75%, changing from 5 to 11 GHz, and amplitude and phase imbalances were optimized to ±0.35 dB and ±7°, respectively.

A numerical analysis using the FEM for an SIW T-junction was demonstrated in [21] at the V-band. The FEM allowed for complex geometries to be solved by dividing the entire structure into smaller subsections. An acceptable agreement was found between the 2D FEM method and CST simulation over the bandwidth from 42.5 to 65 GHz. A differential dual-end feed network was proposed in [22] that incorporated the SIW identical corporate splitter for 24-GHz vehicle applications, following the design presented in [9]. In that work, due to the nonscanning array antennas consisting of traveling-wave propagation, a dual-end feed network was used for a wider bandwidth and gain. Additionally, by offsetting the outermost T-junction, a differential excitation was realized, and, to avoid monopulse radiation at the lower frequencies, a simple filter with vias was applied to the outermost T-junction.

An enhanced cophase bandwidth SIW hybrid power divider was reported in [23] at the X-band. In that work, the optimum design guidelines of the power divider were provided where the number of split (M) was not a power of 2. The reported configuration was transversely symmetrical and included five conventional two-way dividers and two hybrid three-way dividers. The hybrid three-way dividers consisted of one Y- and one T-divider. The center tuning via position was responsible for the power division, and the corner tuning vias at the SIW bends were for matching the output ports. For unequal division, the phase compensation was achieved by offsetting the input window for the conventional dividers, and 180° phase shifters were used for hybrid dividers. That work reported 2% phase bandwidth with ±7° imbalance and 4% with ±13° imbalance.

Recently, a low-sidelobe SIW longitudinal slotted array antenna incorporating a broadband unequal feeding network was proposed in [24] for 5G handset devices. In that work, an eight-way broadband power divider was proposed, consisting of one uniform and three nonuniform T-dividers and a novel method for phase compensation, which did not require any change in the path lengths. Taylor beam-pattern synthesis was applied to obtain different weighting ratios to achieve the lower sidelobe level (SLL). The design process for the novel nonuniform T-divider was divided into three steps. First, a conventional uniform T-divider, as shown in Figure 9, with appropriate impedance matching was designed. The power difference was found to be proportional to the change of P_1 in the x-direction until approximately 10 dB, resulting in phase mismatch between ports 2 and 3. Second, phases were matched by moving the group posts (P_1 and P_2) rather than changing the path lengths. The impedance matching was disrupted after this step due to the postposition change. Once the phases were matched, the impedance matching was improved by optimizing the three post positions in the last step. The Y-divider has pursued the same process for nonuniform designs. Following the steps, two nonuniform T-dividers were designed with $|\Delta\text{out}| = |S_{31} - S_{21}|$ of 6 and 9 dB, with fractional bandwidth of 33% and 31%, respectively. A wider bandwidth can be achieved with this technique for higher SLLs, but phase compensation would be a challenge for a higher split ratio.

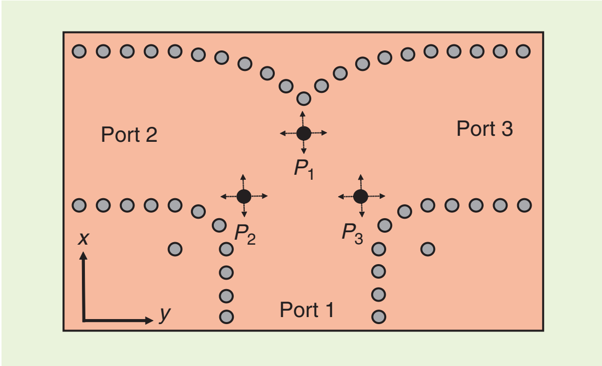

FIGURE 9. The nonuniform T-dividers.

MULTILAYER CONFIGURATIONS

The overall size of the conventional corporate topology can be reduced by introducing multilayers with coupling slots for vertical integration. An 8 × 10 SIW slot antenna array presented in [11], incorporating an eight-way single-layer corporate feed network at the K_u-band, allowed the overall antenna size to be reduced to half through use of the multilayered structure in [25], engrafting a coupling slot between the layers. The position and size of the coupling slot were optimized following the guidelines from [26] to obtain a better coupling level, with an insertion loss of approximately 1 dB. A similar multilayered approach was followed to design four- and eight-way power dividers at the K_a-band in [27], with the length reduced to half as compared to the design in [9]. Moreover, depending on the application, antenna bandwidth and gain enhancement were also performed by introducing an SIW cavity where the mulilayer structures were implemented [28], [29]. The cavity not only supresses the surface wave but also acts as a radiating element, thereby increasing radiation efficiency and further improving gain.

A single-layer SIW feed network incorporated with only wideband T-junctions for a 4 × 4 multilayered cavity-backed aperture-coupled patch antenna array was presented in [30] for V-band applications. Despite the radiating-slots performance, the feed network was found to be complex due to the multiple rows of vias required in a single wall to minimize the radiation leakage. In response to the design complexity, a multilayered compact SIW that incorporated the feed network for 256 antenna array elements was proposed in [31], inspired by [32] and [33]. The proposed power-divider structure was divided into two layers. The first layer consisted of the power split for 64 coupling slots, which is a similar design to [30], excluding the multiple via lines in a single via wall. The second layer included 64 sets of a 2 × 2 subarray split for 256 radiating elements, including one coupling slot in each 2 × 2 subarray to couple the power from layer 1 to layer 2. An example of this configuration for 64 radiating elements is illustrated in Figure 10.

A two-way multilayered alternating SIW power divider with low-temperature cofired ceramic (LTCC) technology for high-desity integration was proposed in [34]. The proposed design realized a longitudinal coupling slot for vertical transition. The coupling slot length was mentioned to be the only optimizing parameter for achieveing a better coupling level. Significant disagreement was found in the transmission coefficient, possibily due to reduction of the post fire shirnkage percentage of the LTCC module. Multilayered SIW E-plane power dividers were proposed in [35] for X-band applications. The coupling between the SIW and microstrip through coupling slots was also investigated in [36], with adequate impedance matching and good isolation achieved. To summarize, multilayered dividers seem to be useful for the large antenna array feed designs at

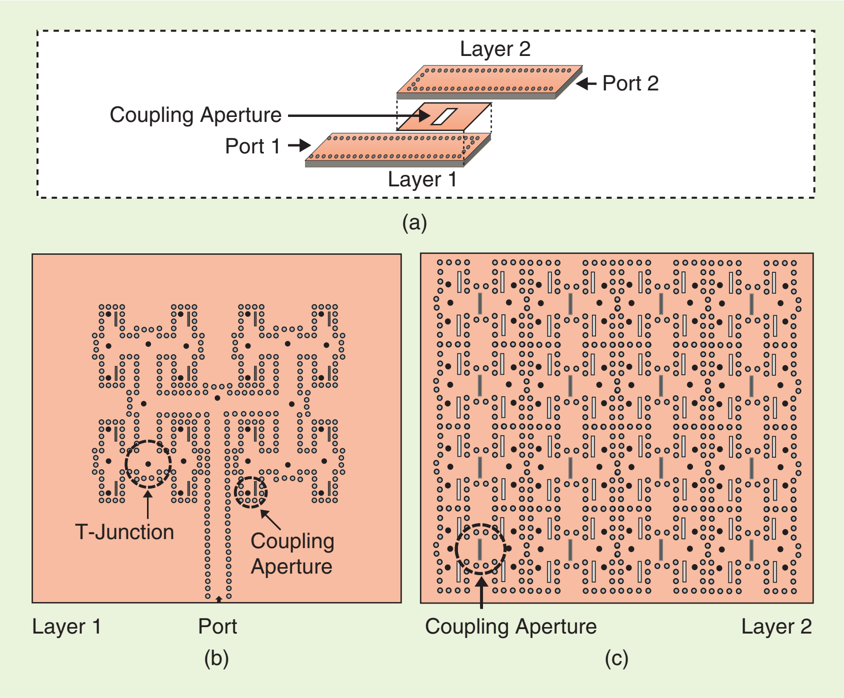

FIGURE 10. (a)–(c) A multilayer SIW corporate feed network configuration/topology.

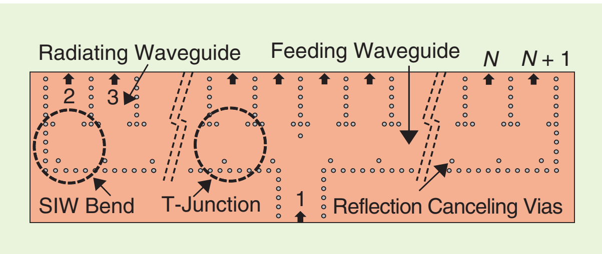

FIGURE 11. An SIW *N*-way series feed network configuration.

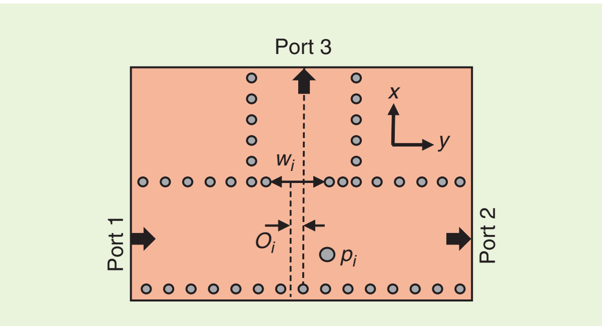

FIGURE 12. A T-junction for a series divider.

higher frequency, ensuring structural compactness. Additionally, designers get the freedom of adding more layers per cavity for antenna gain enhancement and can also apply beam tapering algorithms in a planar configuration.

Multilayer assembling needs to be performed carefully to avoid unwanted losses during coupling. In connection with the literature from SIW corporate power dividers, the following points can be noted.

- The SIW corporate structure comprises three fundamental blocks: the T-junction, Y-junction, and SIW bends. Discontinuities from these junctions must be taken care of to achieve lower reflection from multistages.
- In the Y- and T-junctions, optimization of the inductive post position can minimize reflections and function as a determinant for achieving both equal and unequal split ratios [23].
- Arc-swept SIW bends [13], [24] demonstrated lower reflection with proper selection of bend angle compared to the right angle and bends with inductive posts.
- Multilayered configurations can be a suitable option at higher-frequency designs, that is, for lower SIW widths and also for the compactness of the conventional SIW power-divider designs [31].

SERIES DIVIDERS

Series structure has been adopted in SIW power-divider design due to its key advantages of compactness and lower insertion loss. As the signal needs to travel a shorter path compared to the corporate feed, the insertion loss and radiation leakage are found to be lower. Figure 11 shows the general configuration of a multiway SIW series power divider. The multiway power divider comprises several T-junctions with SIW bends at the two corners. Reflection-canceling vias are placed to improve the impedance matching. An SIW six-way series power divider was presented in [37] for a dual-polarized slot antenna at the 25-GHz band. In that work, several T-junctions were cascaded to form a multiway power divider and the adjoining T-junctions seperated by a guide-wavelength distance to match the phases of all of the ports. However, the cophase bandwidth of the proposed power divider was found to be inconsistent with the frequency. Consequently, an unbalanced pattern bandwidth in the E-plane can be expected, which was not reported in the article. Alternating phase 2 SIW series power dividers (eight way and 16 way) were reported in [38] for the X-band. A nonuniform power division algorithm has been applied to the divider designs for the antenna sidelobe reduction. From the T-junction structure shown in Figure 12, the x and y positions of the center via p_i can be optimized to suppress the reflection, the required unequal power ratio can be obtained by varying the width w_i, and the port phases can be slightly adjusted by offsetting O_i.

Apart from the advantages of compact size, external mutual coupling was found to be high due to lower cophase bandwidth of the power divider that also resulted in broadened beamwidth at the E-plane. A four-way series divider was proposed for a 4 × 20 SIW slot antenna for K_a-band traffic-monitoring radar applications [39]. T-junctions and SIW bends were optimized, and a better cophase bandwidth was observed. Nevertheless, the pattern bandwidths in both the E- and H-planes were not reported in that work. A 12-way nonuniform series divider [40] adapting the Dolph–Chebyshev distribution algorithm for –25-dB SLL and a 16-way uniformly distributed series divider [41] were presented for K-band applications. The pattern bandwidths in both the E- and H-planes were presented in both works [40] and [41], and an optimal coherent pattern was observed. Finally, a wideband cavity-backed SIW slot antenna incorporated with a four-way series feed network was presented in [42].

Despite its compactness, a series feed network exhibits lower cophase bandwidth, making it frequency sensitive. As the frequency varies, the antenna beam tends to tilt. Such an attribute can be utilized in frequency-scanning arrays but is usually undesirable. In addition, external mutual coupling was found to be high, which resulted in convergence during array synthesis.

MMI

The MMI power dividers based on the self-imaging principle [43], [44] are quite popular in photonic integrated circuits for optical communication due to their robust performance in terms of polarization and wavelength variations as well as their fabrication flexibilities. Later, such a concept was embedded into graded indexed waveguides, where the single or multiple images of the input field were reproduced at periodic intervals along the direction of propagation, as a consequence of multimodal interference. The MMI-based N-way power dividers consist of two parts: monomode (access) and multimode SIWs. In comparison with the series structure, the feeding waveguide dimension is laterally increased to support multiple modes. A single image of the input is formed at $z = p(3L_\pi)$ distance, while multiple (N) images can be generated at $z = p(3L_\pi)/N$ with equal amplitudes of $1/\sqrt{N}$ but distinctive phases, as shown in Figure 13 [44].

A six-way MMI SIW power divider (equal split) was proposed in [45] to operate at 25 GHz. Due to the absence of cascaded multistages compared to series or corporate feed networks, the insertion loss was 1.2 dB lower than the theoretical value for split ratio of 1:6. Although the amplitude looks nicely balanced at the operating frequency, it varies extensively as the frequency changes, which makes the return loss and cophase bandwidth narrower; in addition, the maximum phase difference was approximately 90° between output ports.

An improved eight-way MMI power divider with unequal split ratio was reported in [46]. The split ratio was targeted to achieve –20 dB using the Taylor distribution method. Phase shifters were adjoined to improve the cophase bandwidth. Apart from the benefits of lower insertion losses, the MMI method lacks compactness and bandwidth, which requires additional investigation.

HMSIW

The HMSIW concept was first proposed by Hong et al. [50], attempting to reduce the SIW structural size by 50% to obtain more freedom in designing miniaturized multiport networks. As the SIW structure exhibits a large width-to-height ratio, which makes the TE_{10} the dominant mode, the maximum value of the E-field is found at the vertical center plane along the direction of propagation. Accordingly, the center plane can be considered as a magnetic wall. Thus, bifurcating the SIW along the propagation direction allows keeping the mode intact, which was called *HMSIW*, as shown in Figure 14(a). The first HMSIW T-junction and two classes of multiport design were reported in [47]. The T-divider functioned as a fundamental block for the multiway divider, where the air gap was placed between the output ports to ensure an equal split ratio. In addition, a row of vias were placed to protect the dominant mode from distortion. A four-way HM series divider was designed with insertion loss of 0.6 dB, which was further improved to 0.4 dB with another hybrid design method. An unequal split ratio can also be

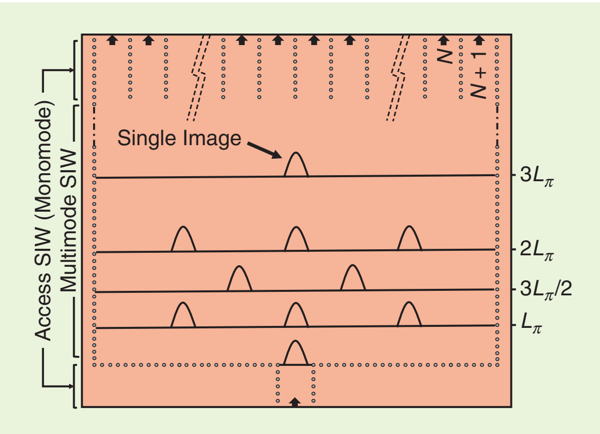

FIGURE 13. The MMI configuration.

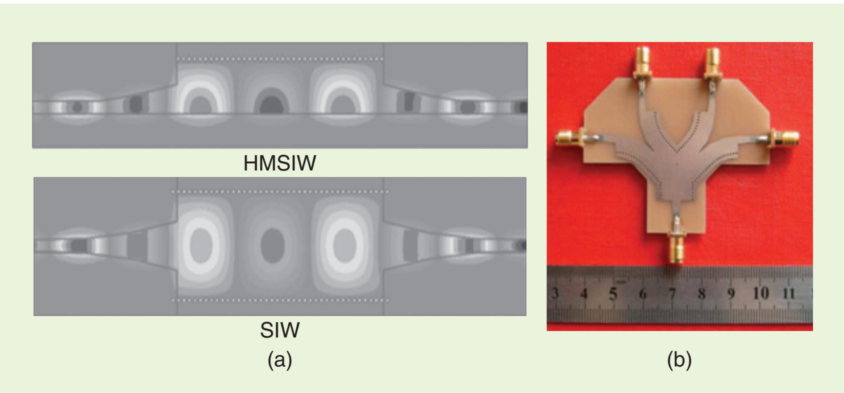

FIGURE 14. The HMSIW configuration and power splitter: (a) TE_{10} mode in HMSIW [47] and (b) a four-way divider [48].

obtained with the proposed design by varying the air gap. A compact multilayer HMSIW alternating-phase power divider was presented in [51] for the X-band. An insertion loss of 1 ± 0.5 dB was reported, and further resistive coupling slots were employed between output ports, which improved the isolation by 15 dB and 20 dB for the lateral and diagonal ports, respectively [52]. An image-transition method was proposed in [53] to obtain structural symmetry, which is absent in HMSIW, and three T-junction types associated with the proposed method were presented and validated with measured results. However, significant phase imbalance was observed over the operating bandwidth. A 90° HMSIW Y-junction was reported in [48] along with a four-way divider, as shown in Figure 14(b). The classical waveguide theory on the inductive post was applied to suppress the port reflections. Apart from the merits of compactness and lower losses, HWSIW power-divider performance was degraded due to lower cophase bandwidth when used as series dividers. Limited research has been performed on the unequal-split balanced-phase category, leaving a room for research on transition-network designs.

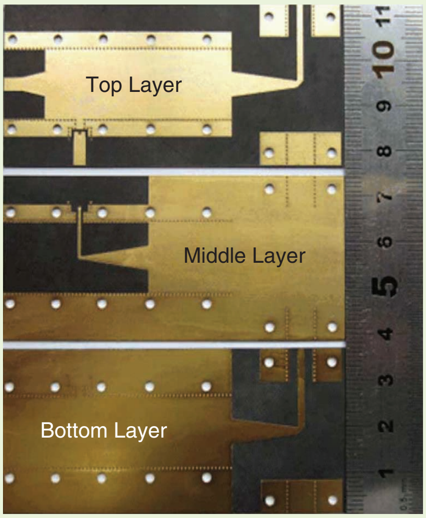

FIGURE 15. The HMSIW magic-T [49].

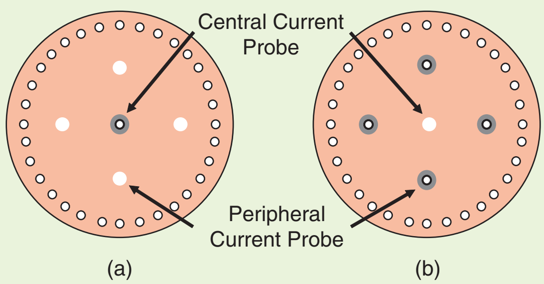

FIGURE 16. An SIW radial-cavity power divider (four-way): (a) the top and (b) bottom views.

MAGIC-T

Magic-T is one of the key components of microwave integrated circuits, such as power dividers, mixers, and antenna feed networks. The traditional magic-T is a 3D waveguide structure, which is basically a combination of hybrid E- and H-plane junctions. To realize such a topology in planar form, first a slotline-to-SIW transition was proposed in [54] at the X-band. While transmitting the signal from slotline to SIW, the electric field polarization changes from the horizontal to vertical orientation. The proposed transition network was utilized to design a magic-T network, which achieved insertion losses of 0.6 dB (in phase) and 0.7 dB (out of phase) as well as amplitude and phase imbalances of 0.2 dB and 1.5°, respectively.

The conventional magic-T suffers from larger size and lower fractional bandwidth, which is usually not more than 10%. An improved configuration was reported in [55] and [56], where 75% of the overall size was reduced using the HM technique, and the fractional bandwidth was improved to 18.3%. As shown in Figure 15, port 1 was considered as the difference (E) port and port 4 as the sum (H) port of the magic-T formation, while the other ports were power-dividing arms. The slotline was terminated with a radial stub to obtain broadband-mode conversion and reduce the circuit size. Moreover, the amplitude and phase balances were carefully taken into account, with imbalances of less than 0.23 dB and 2°, respectively.

To achieve broadband response, another design introducing stripline-to-SIW was presented in [49], with improved bandwidth up to 49.1%. An impressive isolation of 40 dB between ports 1 and 4 was reported in that work. Different approaches, such as a higher-order-mode cavity [57], coupling slot [58], and one-third-mode substrate-integrated resonator [59] have also been reported to improve the magic-T performance in terms of bandwidth, isolation, amplitude, and phase imbalances.

RADIAL CAVITY

Radial-cavity-resonant SIW power dividers exhibit significant reduction in insertion loss and ensure compact size for single-stage *N*-way power division. An SIW radial cavity is a dielectric-filled planar form of the radial waveguide, comprising metallic vias to actualize a circumferential wall of electric fields, where the adjacent equivalent waveguides are separated by magnetic walls. Song et al. [60] first introduced the idea of radial-cavity power dividers in the SIW domain through the design of a four-way power divider at the K_u-band, as shown in Figure 16. As current probes were used to feed the radial cavity through a coaxial cable, the metallic vias were exerted to place the identical central and peripheral probes to accommodate current probes. A minimum insertion loss of 0.6 dB at the center frequency and –10 dB bandwidth of 1.4 GHz was achieved. Another similar topology for an eight-way power divider at the K_a-band was reported in [61]. Although the proposed design produced an excellent power-combining efficiency of 84%, it had lower bandwidth and higher insertion losses.

An equivalent circuit model was developed, and the design guidelines were reported in [62] through the design of an eight-way radial-cavity power divider at the C-band. The insertion loss was effectively reduced to 0.2 dB, and an acceptable phase imbalance was observed; however, a lower bandwidth was also observed. A four-way differential SIW radial power combiner was presented in [63] for S-band applications. The 180° out-of-phase response at the adjacent ports was obtained by flipping the current probes, which changed the electric field polarities. Excellent insertion loss and power balance were obtained, but the bandwidth was significantly lower. In response to this issue, an improved wideband (approximately 78%) eight-way out-of-phase power divider was reported in [64]. Better impedance matching and improved rejection band were achieved by introducing a hybrid multivia probe and multiple radial slots.

The narrow bandwidth of the radial-cavity type was caused by the resonant structure, which was further improved by substrate-integrated-rectangular-waveguide (SIRW) power dividers. The *N*-way power-divider topology incorporated with the SIRW technique was initiated in [67] through a four-way divider design at the X-band. Similar current-probe coaxial feeding was used where the central and peripheral probes were separated by $n{\cdot}\lambda_g/2$, and the distance between the peripheral probe and short wall was $\lambda_g/4$. A wideband response with lower insertion loss was reported. An improved model was reported in [68], where the bandwidth was increased up to 70% by using a dual-disk central probe. Unequal power division and a phase compensation technique for the SIW radial-cavity power divider was reported in [69]. An additional set of vias, s_1, was added to improve the transition between the TEM (by coaxial cable) and TE modes (SIW radial cavity), which was affected by the lower height of inserted coaxial cable. The angle α was set to 45° for equal power split and further varied to obtain unequal split. The imbalanced phases due to unequal split were controlled by introducing the s_2 set of vias. The maximum power difference of 2.94 dB with a phase imbalance of 2.3° was achieved.

WILKINSON AND GYSEL DIVIDERS

Several applications require higher isolation between the output ports of power dividers or combiners. For example, the antenna feed network with higher isolation blocks the interelement interferences. Wilkinson power dividers, including a lossy network or resistive branch between ports, ensure good isolation [Figure 17(a)]. The first HMSIW Wilkinson power divider was reported in [70] with an improved port isolation better than –10 dB. As the HMSIW does not support higher-order modes, such as TE_{20}, the bandwidth increased by up to 86%. Later, another approach was initiated [52] in designing a Wilkinson HMSIW splitter, which improved the isolation by modifying the transition network instead of the divider structure.

Meanwhile, a new technique was presented in [65], in which the magic-T configuration was adopted with a matched E-plane arm. Due to the matched E-plane arm, the magic-T worked as a three-port power splitter with higher isolation, which was designed by placing multiple terminating resistors on an etched slot along the electric field direction on the upper conducting layer. A maximum isolation of 15 dB and return-loss bandwidth of 42% were reported. A ring-shaped Wilkinson power divider was proposed in [71], addressing the impedance variation method without affecting the cutoff frequency and optimal process for integrating the resistors. However, due to the unavoidable parasitic capacitance of resistors, Wilkinson splitters are mostly suitable for low-power applications.

A Gysel power divider [Figure 17(b)], consisting of an HMSIW and microstrip isolation network with higher power-handling capability, was presented in [66] and [72]. The even–odd mode technique was applied for the analysis, and metallic vias were replaced with slots for higher design efficiency. The overall size was reduced by connecting 50-Ω resistors to ground, which replaced two isolation ports. An insertion loss of 4.1 dB and minimum phase imbalance of 5° were obtained. In the case of high power requirements, Gysel dividers are appropriate but require further investigation.

PERFORMANCE ANALYSIS

The previous section detailed the progressive development of SIW power dividers over the past decade. This section provides a performance analysis of all mentioned divider types, which will help designers select the appropriate power divider for their specific applications and required future development. Table 1 lists the key parameters of the power dividers.

Ideally, an appropriate power divider is expected to exhibit a wide bandwidth along with lower insertion loss. In addition, the cophase bandwidth indicates performance sustainability over the return-loss bandwidth. The structural compactness is also important to meet the overall system housing requirements. Significant improvements have been spotted on bandwidth enhancement and insertion-loss minimization. Corporate, series, and MMI power dividers are of quite similar structures and are mostly applied to antenna feed networks, but they differ in terms of return loss and cophase bandwidth performances. Series and MMI power dividers have lower insertion loss along with compact size, but they exhibit lower return-loss bandwidth (<10%). In contrast, corporate dividers exhibit a wider return-loss bandwidth of up to 75% as well as wider cophase bandwidth. Although the corporate structure has a larger size, it provides more freedom

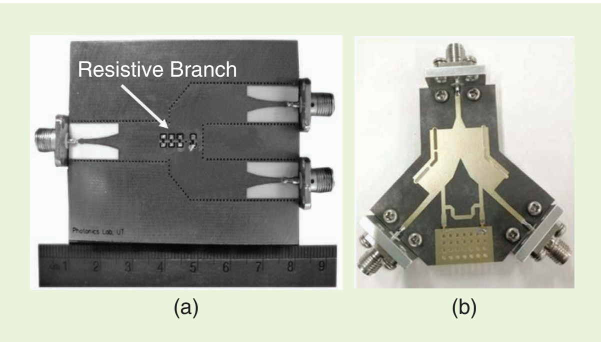

FIGURE 17. The SIW (a) Wilkinson [65] and (b) Gysel [66] power dividers. {Source: (a) [65]; used with permission.}

TABLE 1. THE PARAMETERS FOR DIFFERENT SIW POWER DIVIDERS.

Category	Reference	Split Number	Ratio Bandwidth (%)	Insertion Loss (dB)	Imbalance Amplitude (dB)	Imbalance Phase (°)
Corporate	[9]	16	16	14.5	±0.5	—
	[20]	8	75	10.7	±0.35	±7
	[31]	4	24	6.15	±1	—
Series	[37]	3	>6	~4.6	±0.5	180 ± 1
	[73]	12	>5	~12	±0.5	180 ± 15
MMI	[45]	6	8	9	±0.4	±90
HMSIW	[47]	4	25 (hybrid)	6.4	—	—
	[51]	4	37	7	±0.5	180 ± 2.5
	[53]	2	28 (type 1)	3.3	4.1 ± 0.5	73 ± 8
Magic-T	[54]	2	11	3.7	±0.2	±1.5
	[55]	2	18.9	3.85	±0.23	±2
	[49]	2	49.1	3.85–4.6	±0.24	±3
Radial cavity	[63]	4	8.7	6.15	±0.03	±1
	[64]	8	78	9.3	±0.3	±3
	[74]	7	45	3.4	—	±24
	[67]	4	42	6.6	—	—
	[68]	4	70	6.37	—	—
Wilkinson (Isolation > 10 dB)	[70]	2	86	~3.5	—	—
	[65]	2	42	~4.5	—	—
Gysel (Isolation > 20 dB)	[72]	2	4.82–9.38	4.2–4.4	±0.1	±2.5–5.5

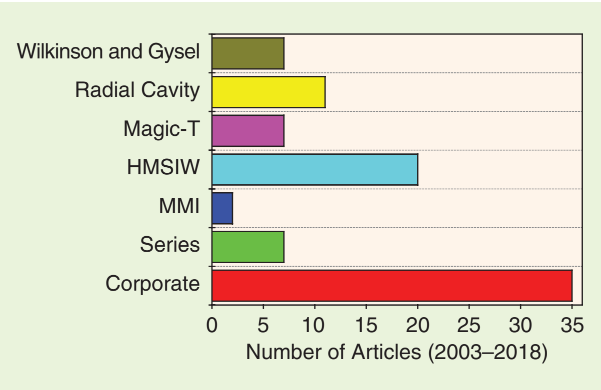

FIGURE 18. The research progress on SIW power dividers.

in designing both uniform and nonuniform split ratios with balanced amplitude and phase. Additionally, structural compactness can also be achieved in the corporate structure with a multilayered configuration.

HMSIW dividers are popular for their compactness, which is approximately half of the regular SIW size with lower insertion loss. A potential challenge with HMSIW dividers is to keep the modal behavior intact while integrating several T-junctions to achieve the required number of splits. The HMSIW formation is also adopted in designing the SIW magic-T, where several attempts at improving the multilayer coupling methods have been observed to achieve better vertical coupling. Investigation of bandwidth enhancement and output balancing seems to be a significant aspect of magic-T topology.

Radial-cavity dividers are useful for multiport networks, that is, couplers and mixers. Limited attempts have been reported in the literature, and more investigation is required to understand the practical integration complexities. Wilkinson dividers are reported to serve for the application, which requires higher port isolation. Due to the low-power lossy branch (resistors), the Gysel technique has recently come onboard to improve the power handling capability of this type of divider. Although higher isolation is reported for Gysel dividers, it shows lower bandwidth, which is less than 6% where more attention is needed. The bar chart shown in Figure 18 depicts the number of research articles published on different SIW power dividers in the last 16 years. The corporate network has received the most attention compared to all of the others, possibly due to its direct application for antenna feed systems. However, the other divider topologies require more attention to bandwidth enhancement, loss minimizations, innovation of coupling methods, phase-balancing techniques, and practical integration issues with other system counterparts.

An example is the passive microwave radiometer (PMR) system, which is used to determine soil moisture content for improving irrigation efficiency. A phased array antenna is one of the vital blocks of that PMR system, and power dividers are one of the elementary blocks of phased array antennas. Additionally, a lower SLL for the antenna is also a requirement for such application and can be obtained by using nonuniform power dividers with balanced phase. For a linear array antenna, either corporate or series dividers can be the right choice. Although both of the techniques are capable of delivering nonuniform power distribution to the antenna elements, as observed from the literature, the corporate network has a higher return-loss bandwidth. Also, series dividers exhibit lower cophase bandwidth, which could be the reason for the undesirable antenna beam-squint. In comparison, the corporate structure provides higher cophase bandwidth, which makes corporate dividers more suitable for this application.

FINAL REMARKS

This article presented a comprehensive review of different SIW power dividers and described their development over the past decade. Due to the immense demand for developing mm-wave circuits and systems, an efficient power divider/combiner is required where SIW technologies significantly established their vestige. Such an SIW technique merged the advantages of the conventional rectangular waveguide and microstrip, eliminating of the drawbacks of both. However, more investigations are required of practical integration and fabrication issues, which can potentially amplify the scope of SIW technology on power-divider designs.

ACKNOWLEDGMENTS

This work was supported by the Australian Research Council under the grant DP160104233.

AUTHOR INFORMATION

Shahriar Hasan Shehab (shahriar.shehab@monash.edu) is pursuing his doctoral degree with the Monash Microwave, Antennas, RFID, and Sensors research group at Monash University, Australia. His research interests include substrate-integrated-waveguide technology, phased array antennas, telematics, and satellite communication.

Nemai Chandra Karmakar (nemai.karmakar@monash.edu) is an associate professor in the Department of Electrical and Computer Systems Engineering, Monash University, Australia. He has more than 20 years of teaching, design, and development experience in antennas, microwave active and passive circuits, and radio-frequency identification in Canada, Australia, and Singapore.

Jeffrey Walker (jeff.walker@monash.edu) is a professor and the head of the Department of Civil Engineering at Monash University, Australia. His research interests include soil moisture remote sensing and data assimilation, including development of the only Australian airborne capability for simulating new satellite missions for soil moisture.

REFERENCES

[1] D. Deslandes, "Design equations for tapered microstrip-to-substrate integrated waveguide transitions," in *Proc. Microwave Symp. Dig. (MTT), 2010 IEEE MTT-S Int.*, pp. 704–707.
[2] F. Shigeki, "Waveguide line (in Japanese)," Japan Patent 06-053, 1994.
[3] J. Hirokawa and M. Ando, "Single-layer feed waveguide consisting of posts for plane TEM wave excitation in parallel plates," *IEEE Trans. Antennas Propag.*, vol. 46, no. 5, pp. 625–630, 1998.
[4] J. Volakis, *Antenna Engineering Handbook*, 4th ed. New York: McGraw-Hill, 2007.
[5] F. Xu and K. Wu, "Guided-wave and leakage characteristics of substrate integrated waveguide," *IEEE Trans. Microw. Theory Techn.*, vol. 53, no. 1, pp. 66–73, 2005.
[6] Y. Cassivi, L. Perregrini, P. Arcioni, M. Bressan, K. Wu, and G. Conciauro, "Dispersion characteristics of substrate integrated rectangular waveguide," *IEEE Microw. Compon. Lett.*, vol. 12, no. 9, pp. 333–335, 2002.
[7] H. Uchimura, T. Takenoshita, and M. Fujii, "Development of a 'laminated waveguide'," *IEEE Trans. Microw. Theory Techn.*, vol. 46, no. 12, pp. 2438–2443, 1998.
[8] S. Germain, D. Deslandes, and K. Wu, "Development of substrate integrated waveguide power dividers," in *Proc. Canadian Conf. Electrical and Computer Engineering 2003 (CCECE 2003)*, vol. 3. Montréal, Canada: IEEE, pp. 1921–1924.
[9] Z. Hao, W. Hong, H. Li, H. Zhang, and K. Wu, "Multiway broadband substrate integrated waveguide (SIW) power divider," in *Proc. 2005 IEEE Antennas and Propagation Society Int. Symp.*, vol. 1. Washington, D.C.: IEEE, pp. 639–642.
[10] Z. C. Hao, W. Hong, J. X. Chen, X. P. Chen, and K. Wu, "A novel feeding technique for antipodal linearly tapered slot antenna array," in *Proc. IEEE MTT-S Int. Microwave Symp. Dig.*, 2005, p. 3.
[11] D. Navarro, L. Carrera, and M. Baquero, "A SIW slot array antenna in Ku band," in *2010 Proc. 4th European Conf. Antennas and Propagation (EuCAP)*, pp. 1–4.
[12] S. S. Karimabadi and A. R. Attari, "Broadband substrate integrated waveguide four-way power divider," in *Proc. IEEE 2012 6th Int. Symp. Telecommunications (IST)*, pp. 80–83.
[13] C. Yu, W. Hong, and Z. Kuai, "Substrate integrated waveguide power divider fed dual-dipole array antenna," *J. Electromagn. Eng. Sci.*, vol. 10, no. 3, pp. 171–174, 2010.
[14] B. Liu et al., "Substrate integrated waveguide (SIW) monopulse slot antenna array," *IEEE Trans. Antennas Propag.*, vol. 57, no. 1, pp. 275–279, 2009.
[15] Y. J. Cheng, W. Hong, and K. Wu, "94 GHz substrate integrated monopulse antenna array," *IEEE Trans. Antennas Propag.*, vol. 60, no. 1, pp. 121–129, 2012.
[16] R. Kazemi, R. A. Sadeghzadeh, and A. Fathy, "A new compact wide band 8-way SIW power divider at X-band," in *Proc. 2011 Loughborough Antennas and Propagation Conf.*, pp. 1–4.
[17] R. Kazemi, A. E. Fathy, and R. A. Sadeghzadeh, "Ultra-wide band vivaldi antenna array using low loss SIW power divider and GCPW wide band transition," in *Proc. 2012 IEEE Radio and Wireless Symp.*, pp. 39–42.
[18] A. P. Wirawan, P. H. Mukti, and E. Setijadi, "Design of substrate integrated waveguide based power divider for S-band applications," in *Proc. 2015 Int. Conf. Radar, Antenna, Microwave, Electronics and Telecommunications (ICRAMET)*, pp. 28–31.
[19] G. Tan, S. Ibrahim, and M. Razalli, "24GHz Substrate Integrated Waveguide power splitter for six-port short range radar based sensor," in *Proc. 2016 IEEE Asia-Pacific Conf. Applied Electromagnetics (APACE)*, pp. 113–116.
[20] R. Kazemi and A. E. Fathy, "Design of single-ridge SIW power dividers with over 75% bandwidth," in *Proc. 2014 IEEE MTT-S Int. Microwave Symp. (IMS2014)*, pp. 1–3.
[21] F. Benzerga, M. Abri, H. A. Badaoui, J. Tao, and T. H. Vuong, "1-2 SIW power dividers modeling using a rigorous finite element method for V-band applications," in *Proc. 2015 9th Jordanian Int. Electrical and Electronics Engineering Conf. (JIEEEC)*, pp. 1–5.
[22] H. Zhou and W. Hong, "45° Polarized slot array antenna with differential dual-end feeding network for vehicle applications," in *Proc. 2015 IEEE Int. Symp. Antennas and Propagation (ISAP)*, pp. 1–3.
[23] H. Yang, G. Montisci, Z. Jin, Y. Liu, X. He, and G. Mazzarella, "Improved design of low sidelobe substrate integrated waveguide longitudinal slot array," *IEEE Antennas Wireless Propag. Lett.*, vol. 14, pp. 237–240, Jan. 2015.
[24] S. J. Park, D. H. Shin, and S. O. Park, "Low side-lobe Substrate-Integrated-Waveguide antenna array using broadband unequal feeding network for millimeter-wave handset device," *IEEE Trans. Antennas Propag.*, vol. 64, no. 3, pp. 923–932, 2016.
[25] D. Navarro-Méndez, L. Carrera-Suárez, M. Baquero-Escudero, and V. Rodrigo-Peñarrocha, "Two layer slot-antenna array in SIW technology," in *Proc. 2010 IEEE European Microwave Conf. (EuMC)*, pp. 1492–1495.

[26] A. Suntives and R. Abhari, "Transition structures for 3-D integration of substrate integrated waveguide interconnects," *IEEE Microw. Compon. Lett.*, vol. 17, no. 10, pp. 697–699, 2007.
[27] X. Zhongshan, B. Liu, Z. Yongjiu, T. Bo, and J. Shengli, "A novel Ka band multi-layer SIW power divider," in *Proc. 2011 Cross Strait Quad-Regional Radio Science and Wireless Technology Conf.*, vol. 1. Harbin, China: IEEE, pp. 634–636.
[28] Y. Zhang, Z. N. Chen, X. Qing, and W. Hong, "Wideband millimeter-wave substrate integrated waveguide slotted narrow-wall fed cavity antennas," *IEEE Trans. Antennas Propag.*, vol. 59, no. 5, pp. 1488–1496, 2011.
[29] K. Gong, Z. N. Chen, X. Qing, P. Chen, and W. Hong, "Substrate integrated waveguide cavity-backed wide slot antenna for 60-GHz bands," *IEEE Trans. Antennas Propag.*, vol. 60, no. 12, pp. 6023–6026, 2012.
[30] Y. Li and K.-M. Luk, "Low-sost high-gain and broadband Substrate-Integrated-Waveguide-fed patch antenna array for 60-GHz band," *IEEE Trans. Antennas Propag.*, vol. 62, no. 11, pp. 5531–5538, 2014.
[31] Y. Li and K.-M. Luk, "60-GHz Substrate Integrated Waveguide fed cavity-backed aperture-coupled microstrip patch antenna arrays," *IEEE Trans. Antennas Propag.*, vol. 63, no. 3, pp. 1075–1085, 2015.
[32] Y. Miura, J. Hirokawa, M. Ando, Y. Shibuya, and G. Yoshida, "Double-layer full-corporate-feed hollow-waveguide slot array antenna in the 60-GHz band," *IEEE Trans. Antennas Propag.*, vol. 59, no. 8, pp. 2844–2851, 2011.
[33] J. Xu, Z. N. Chen, X. Qing, and W. Hong, "Bandwidth enhancement for a 60 GHz substrate integrated waveguide fed cavity array antenna on LTCC," *IEEE Trans. Antennas Propag.*, vol. 59, no. 3, pp. 826–832, 2011.
[34] H. Abuzaid, A. Doghri, K. Wu, and A. Shamim, "SIW based multilayer transition and power divider in LTCC technology," in *Proc. 2013 IEEE MTT-S Int. Microwave Symp. Dig. (IMS)*, pp. 1–3.
[35] P. Mohammadi and S. Demir, "Multi-layer substrate integrated waveguide E-plane power divider," *Progress Electromagn. Res. C*, vol. 30, pp. 159–172, June 2012. [Online]. Available: http://www.jpier.org/PIERC/pierc30/13.12042905.pdf
[36] G. Li, K. Song, F. Zhang, and Y. Zhu, "Novel four-way multilayer SIW power divider with slot coupling structure," *IEEE Microw. Compon. Lett.*, vol. 25, no. 12, pp. 799–801, 2015.
[37] S. Park, Y. Okajima, J. Hirokawa, and M. Ando, "A slotted post-wall waveguide array with interdigital structure for 45/spl deg/linear and dual polarization," *IEEE Trans. Antennas Propag.*, vol. 53, no. 9, pp. 2865–2871, 2005.
[38] J. F. Xu, W. Hong, P. Chen, and K. Wu, "Design and implementation of low sidelobe substrate integrated waveguide longitudinal slot array antennas," *IET Microw., Antennas Propag.*, vol. 3, no. 5, pp. 790–797, 2009.
[39] X.-P. Chen, L. Li, and K. Wu, "Multi-antenna system based on substrate integrated waveguide for Ka-band traffic-monitoring radar applications," in *Proc. IEEE European Microwave Conf., 2009 (EuMC 2009)*, pp. 417–420.
[40] T. Mikulasek, J. Puskely, and J. Lacik, "Design of radome-covered substrate integrated waveguide slot antenna array," in *Proc. IEEE 2013 7th European Conf. Antennas and Propagation (EuCAP)*, pp. 1437–1441.
[41] M. Zhou, Y. Cheng, and W. Huang, "Substrate integrated slot array antenna with required radiation pattern envelope," *Int. J. Antennas Propag.*, vol. 2016, 2016. doi: 10.1155/2016/4031029.
[42] Y. Tian Yang, H. Wei, and Z. Yan, "Wideband millimeter-wave substrate integrated waveguide cavity-backed rectangular patch antenna," *IEEE Antennas Wireless Propag. Lett.*, vol. 13, pp. 205–208, Jan 2014.
[43] H. F. Talbot, "LXXVI. Facts relating to optical science. No. IV," *London, Edinburgh, Dublin Philosoph. Mag. J. Sci.*, vol. 9, no. 56, pp. 401–407, 1836.
[44] L. B. Soldano and E. C. Pennings, "Optical multi-mode interference devices based on self-imaging: Principles and applications," *J. Lightw. Technol.*, vol. 13, no. 4, pp. 615–627, 1995.
[45] N. Yang, C. Caloz, and K. Wu, "Substrate integrated waveguide power divider based on multimode interference imaging," in *Proc. 2008 IEEE MTT-S Int. Microwave Symp. Dig.*, pp. 883–886.
[46] O. Kiris and O. A. Civi, "8 × 4 SIW power divider and slotted array antenna," in *Proc. 2015 IEEE Int. Symp. Antennas and Propagation and USNC/URSI Nat. Radio Science Meeting*, pp. 482–483.
[47] B. Liu, H. Wei, T. Lin, Z. Hong-Bing, J. Wei, and W. Ke, "Half mode substrate integrated waveguide (HMSIW) multi-way power divider," in *Proc. 2006 Asia-Pacific Microwave Conf.*, pp. 917–920.
[48] X. Zou, C. M. Tong, and D. W. Yu, "Y-junction power divider based on substrate integrated waveguide," *Electron. Lett.*, vol. 47, no. 25, pp. 1375–1376, 2011.
[49] F. Zhu, W. Hong, J.-X. Chen, and K. Wu, "Design and implementation of a broadband substrate integrated waveguide magic-T," *IEEE Microw. Compon. Lett.*, vol. 22, no. 12, pp. 630–632, 2012.
[50] W. Hong et al., "Half mode substrate integrated waveguide: A new guided wave structure for microwave and millimeter wave application," in *Proc. IEEE 2006 Joint 31st Int. Conf. Infrared Millimeter Waves and 14th Int. Conf. Teraherz Electronics (IRMMW-THz 2006)*, pp. 219–219.
[51] D. Eom, J. Byun, and H. Y. Lee, "Multi-layer four-way out-of-phase power divider for substrate integrated waveguide applications," in *Proc. 2009 IEEE MTT-S Int. Microwave Symp. Dig.*, pp. 477–480.
[52] D. S. Eom, J. Byun, and H. Y. Lee, "Multilayer substrate integrated waveguide four-way out-of-phase power divider," *IEEE Trans. Microw. Theory Techn.*, vol. 57, no. 12, pp. 3469–3476, 2009.
[53] L. Bing, T. Bo, X. Zhongshang, X. Shuchen, and C. Peng, "A novel image transition in half mode substrate integrated waveguide power divider design," in *Proc. 2011 Cross Strait Quad-Regional Radio Science and Wireless Technology Conf.*, vol. 1. Harbin, China: IEEE, pp. 621–624.
[54] F. F. He, K. Wu, W. Hong, H. J. Tang, H. B. Zhu, and J. X. Chen, "A planar magic-T using substrate integrated circuits concept," *IEEE Microw. Compon. Lett.*, vol. 18, no. 6, pp. 386–388, 2008.
[55] W. Feng, W. Che, and T. F. Eibert, "Compact planar magic-T using half mode substrate integrated waveguide and slotline coupling," in *Proc. 2011 IEEE MTT-S Int. Microwave Symp. Dig. (MTT)*, pp. 1–4.
[56] F. F. He, K. Wu, W. Hong, L. Han, and X. Chen, "A planar magic-T structure using substrate integrated circuits concept and its mixer applications," *IEEE Trans. Microw. Theory Techn.*, vol. 59, no. 1, pp. 72–79, 2011.
[57] P. Wu, S. Liao, and Q. Xue, "A substrate integrated magic-T based on higher order mode cavity and slotline," in *Proc. 2015 Asia-Pacific Microwave Conf. (APMC)*, vol. 2. Nanjing, China: IEEE, pp. 1–3.
[58] J. Huang, G. Hua, B. Cao, and F. Ran, "A 34.5 GHz planar magic-T based on coupling slot and substrate integrated waveguide," in *Proc. 2016 IEEE Int. Conf. Ubiquitous Wireless Broadband (ICUWB)*, pp. 1–3.
[59] F. Xu, C. Zheng, and X. Hu, "Wideband circuits designed on one-third equilateral triangular cavity," in *Proc. 2016 IEEE Int. Workshop on Electromagnetics: Applications and Student Innovation Competition (iWEM)*, pp. 1–3.
[60] K. Song, Y. Fan, and Y. Zhang, "Radial cavity power divider based on substrate integrated waveguide technology," *Electron. Lett.*, vol. 42, no. 19, pp. 1100–1101, 2006.
[61] K. Song, Y. Fan, and Y. Zhang, "Design of low-profile millimeter-wave substrate integrated waveguide power divider/combiner," *Int. J. Infrared Millim. Waves*, vol. 28, no. 6, pp. 473–478, 2007.
[62] K. Song, Y. Fan, and Y. Zhang, "Eight-way substrate integrated waveguide power divider with low insertion loss," *IEEE Trans. Microw. Theory Techn.*, vol. 56, no. 6, pp. 1473–1477, 2008.
[63] Y.-P. Hong, Y.-J. An, and J.-G. Yook, "Differential radial power combiner using substrate integrated waveguide," *Electron. Lett.*, vol. 46, no. 24, pp. 1607–1608, 2010.
[64] K. Song, Y. Mo, S. Hu, Y. Fan, and N. Chen, "Wideband out-of-phase SIW power divider with enhanced stopband," in *Proc. 2013 IEEE Int. Wireless Symp. (IWS)*, pp. 1–3.
[65] K. Sarhadi and M. Shahabadi, "Wideband substrate integrated waveguide power splitter with high isolation," *IET Microw., Antennas Propag.*, vol. 4, no. 7, pp. 817–821, 2010.
[66] H. Chen, X. Wang, W. Che, Y. Zhou, and T. Liu, "Novel Gysel power dividers based on Half-Mode Substrate Integrated Waveguide (HMSIW)," in *Proc. 2018 IEEE MTT-S Int. Wireless Symp. (IWS)*, pp. 1–3.
[67] K. Song, Y. Fan, and X. Zhou, "X-band broadband substrate integrated rectangular waveguide power divider," *Electron. Lett.*, vol. 44, no. 3, pp. 211–213, 2008.
[68] K. Song and Y. Fan, "Broadband travelling-wave power divider based on substrate integrated rectangular waveguide," *Electron. Lett.*, vol. 45, no. 12, pp. 631–632, 2009.
[69] T. Y. Seo, J. W. Lee, C. S. Cho, and T. K. Lee, "Radial guided 4-way unequal power divider using substrate integrated waveguide with center-fed structure," in *Proc. IEEE Asia Pacific Microwave Conf. 2009 (APMC 2009)*, pp. 2758–2761.
[70] Z. Zhen-Yu and W. Ke, "Broadband half-mode substrate integrated waveguide (HMSIW) wilkinson power divider," in *Proc. 2008 IEEE MTT-S Int. Microwave Symp. Dig.*, pp. 879–882.
[71] T. Djerafi, D. Hammou, K. Wu, and S. O. Tatu, "Ring-shaped substrate integrated waveguide wilkinson power dividers/combiners," *IEEE Trans. Compon. Packag. Manuf. Technol.*, vol. 4, no. 9, pp. 1461–1469, 2014.
[72] H. Chen, X. Wang, W. Che, Y. Zhou, and Q. Xue, "Development of compact HMSIW Gysel power dividers with microstrip isolation networks," *IEEE Access*, vol. 6, pp. 60,429–60,437, Oct. 2018.
[73] C. Xiao-Ping, W. Ke, H. Liang, and H. Fanfan, "Low-cost high gain planar antenna array for 60-GHz band applications," *IEEE Trans. Antennas Propag.*, vol. 58, no. 6, pp. 2126–2129, 2010.
[74] C. Rave and A. F. Jacob, "A wideband radial substrate integrated power divider at K-band," in *Proc. 2015 German IEEE Microwave Conf. (GeMiC)*, pp. 84–87.